HortScience 60(8):1400–1408. 2025. https://doi.org/10.21273/HORTSCI18485-25

# Branch-base Angle Influenced the Shoot Growth and Fruit Quality of Flat-type Trellised Pear Trees

**Li Yang, Yin-Sheng Cheng, Zheng Liu, Xie-Yu Li, and Fu-Chen Yang**

*Fruit and Tea Subcenter of Hubei Innovation Center of Agricultural Science and Technology, Wuhan 430064, Hubei, China; and Hubei Key Laboratory of Germplasm Innovation and Utilization of Fruit Trees, Institute of Fruit Tree and Tea, Hubei Academy of Agricultural Sciences, Wuhan 430064, Hubei, China*

**Xian-Shuang Nie**

*College of Horticulture and Gardening, Yangtze University, Jingzhou 434025, Hubei, China*

**Hua Cai and Tao Wu**

*Fruit and Tea Subcenter of Hubei Innovation Center of Agricultural Science and Technology, Wuhan 430064, Hubei, China; and Hubei Key Laboratory of Germplasm Innovation and Utilization of Fruit Trees, Institute of Fruit Tree and Tea, Hubei Academy of Agricultural Sciences, Wuhan 430064, Hubei, China*

*Keywords.* flat-type trellis system, fruit quality, logistic model, pear tree, quadratic equation

***Abstract.*** **Appropriate branch angle is an important technical parameter in the management of new trees to balance vegetative and reproductive growth. However, the effects of different branch angles on shoot growth and fruit quality of pear trees under flat trellis cultivation mode are poorly known. This study was done on *Pyrus pyrifolia* Nakai cv. 'Cuiguan' pear trees using the flat-type trellis cultivation mode in the "Double Primary Branches along the Row" (or, "double-arm") orchard. The three base angles (T1 = 60°, T2 = 30°, T3 = 0°) of 2-year-old branches were tested, and the length and cross-sectional area of branch base (CSAB) of the current-year shoots and fruit quality were monitored over time. The relationship between fruit quality and shoot growth under different treatment conditions was analyzed. The results showed that the length of new shoots decreased in the order T2 > T1 > T3 and that CSAB decreased with an increase in the base angle (T3 > T2 > T1). The rapid growth of current-year shoots started earlier with a decrease in branch angle. The maximum relative growth rate ($v_m$) in CSAB occurred 6.14 days earlier in the T3 than T1 group, with the overall trend being T3 > T2 > T1. In terms of fruit quality, the greatest relative change in daily growth rate regarding fruit weight, transverse and longitudinal diameter, and soluble solids in different treatment groups was recorded between 95 and 110 days after full bloom. The average solid-to-acid ratio in fruit at full maturity was T3 > T2 > T1, titratable acid content was T1>T3>T2 ($P < 0.05$), and the fresh firmness was T1>T3>T2 ($P < 0.05$). There was no significant correlation (at $\alpha = 0.05$) between fruit weight, transverse diameter, longitudinal diameter, soluble solids, and fruit shape index across the treatments. This study clarified the relationship between shoot growth rate and fruit quality formation under different branch-base angles of trellised pear trees, contributing to the improvement of the double-arm pear tree–growing system.**

The pear industry occupies an important position in Chinese agriculture. With the rising labor costs year by year, it is crucial to develop a suitable and efficient cultivation mode. The flat-type trellis "Double Primary Branches along the Row" (also referred to as "double-arm") cultivation mode represents a standardized, low-density, bi-axis pear orchard management approach (Qi et al. 2023; Wu et al. 2014). However, the transformation of pear tree management from three-dimensional to flat trellis cultivation alters the light interception by the leaf canopy and the microenvironment of fruit development, thus influencing tree growth and fruit quality. Under this new cultivation mode, evaluating the effects of different tree management methods on the growth status of fruit trees and predicting their production potential are important issues. The accurate and quantitative simulation analysis of indicators of fruit tree growth and development over time is essential for improving tree management and fruit quality (Rizzolo et al. 2021; Tudela and Santibáñez 2016). Clarifying the relationship between the dynamics of branch growth and fruit quality formation of trellised pear trees can provide a theoretical basis for efficient and high-yield cultivation of pears.

It is common to manage vegetative growth, enhance light utilization rate by the canopy, and improve the productivity of fruit trees by opening the base of branches to keep them at a suitable angle (Jung and Choi 2010; Jung et al. 2012; Samant and Kishore 2021; Zhang et al. 2023). However, different varieties have different physiological responses to the time, or angle, of shoot bending, altering the proportion of long and short branches (Lauri and Lespinasse 2001; Qin et al. 2011). In fruit tree management practices in China, it is common to manipulate branch orientation in the upward vertical direction to regulate vegetative vigor and enhance fruit quality. For example, when the branch angle of 'Pingguo' pear (*Pyrus bretschneideri* Rehd.) trees is maintained at 80° to 90° (i.e., a horizontal angle of ∼0° to 10°), a balance between vegetative growth and fruiting can be achieved (Wu et al. 2008). A branch angle of 60° significantly increases both the yield per branch and per branch group, as well as fruit size in hybrid apricot plum (*Prunus domestica* ×*armeniaca*) (Zhen et al. 2024). In contrast, walnut (*Juglans regia* cv. Lvling) branches positioned above 1.2 m and trained at a 30° angle exhibit greater advantages in terms of fruit yield, average fruit weight, and disease resistance (Ma et al. 2019). Moreover, high-density planting and training systems adopted for the cultivation of European pear (*Pyrus communis* L.) have been reported to significantly improve light utilization and fruit quality by optimizing branch angles and canopy spatial distribution (Musacchi et al. 2021; Sansavini et al. 2008). Collectively, these findings suggest that appropriate branch angle management not only improves nutrient allocation within the tree but also extends the economic lifespan of the orchard.

The mathematical models (e.g., based on polynomial, logistic, or linear equations) are used to simulate and predict the tree growth and changes in various indices in the fruit growth cycle (Peng et al. 2021). Among various models, the univariate polynomial equation was suitable for the growth and development dynamics of apricot (Bao et al. 2007), Taiwan pineapple sakya (Cai et al. 2016), and olive (Yang et al. 2020), whereas the logistic equation could better fit the growth and development dynamics of sour cherry (Hillmann et al. 2021), guava (Panghal et al. 2019), macadamia (Han et al. 2023), and pecan nut (Panta et al. 2023), as well as the changes in metabolites as influenced by environmental conditions (Dai et al. 2009; Genard et al. 1999).

The growth models can determine the key factors influencing the formation of marketable quality fruits and the growth of fruit trees. However, there is a paucity of reports on the growth model of trellised pear trees. Therefore, based on the logistic growth curve and polynomial equations, this study applied treatments with horizontal branch angles of 0°, 30°, and 60° to flat-trellised pear trees and

analyzed the multiple indicators of growth during the development of new shoots and fruits to establish an explanatory mathematical model under different branch-pulling angles. The relationship between the growth rate of shoots and the formation of fruit quality was explored for the first time to provide a scientific basis for improving the standard technology of double-arm trellised pear trees.

## Materials and Methods

### Overview of test site

The experimental site (114°8′55″E, 30° 17′24″N, altitude 30 m) is in Jiangxia District, Wuhan City, Hubei Province (in the area between Jianghan Plain and southern Hubei Hills) and features yellow-brown soil. The site has a subtropical monsoon climate with an annual average temperature between 15.9 and 17.9 °C and an average annual precipitation of 1260.6 mm.

### Experimental material

This experiment was carried out in the double-arm standard trellised pear orchards of the Fruit Tree Tea Research Institute of Hubei Academy of Agricultural Sciences. The test trees species were 4-year-old 'Cuiguan' (*Pyrus pyrifolia* Nakai) grafted onto *Pyrus calleryana* Decne. rootstocks, with 'Wonhwang' pear (*P. pyrifolia* Nakai) used as the pollinator. 'Cuiguan' pear trees with strong and uniform tree vigor were selected, and standardized management was carried out according to the technical regulations of the "Double Primary Branches along the Row Flat Type" standard trellised pear orchard (Wu et al. 2015). All test branches selected in this study were all lateral branches, which, in their natural growth state, formed an angle of ∼20° with the upward vertical axis.

### Experimental design

Three experimental plots were arranged in a double-arm trellised pear orchard (3-m × 4-m spacing, 825 trees/ha). Each experimental plot included eight or nine 'Cuiguan' pear trees (experimental units) with strong growth and consistent tree vigor, (plot a1, 9 trees; plot a2, 9 trees; plot a3, 8 trees) (Fig. 1A). The 2-year-old branches (on each the two main tree arms) with the same orientation, similar diameter, length, and natural growth angle were selected for different treatments. The base angle of 2-year-old branches was fixed in early Feb 2023 (Fig. 1B). The angles were 60° (T1), 30° (T2), and 0° (T3) with respect to the horizontal line (Fig. 2). Each test group (T1 to T3) treated 70 to 100 branches, and the measurement position was marked. The length and diameter of the newly emerged shoots on the branches were measured and recorded at 6- to 10-d intervals. The CSAB measurement was done about 1 cm from the base of the branch, and the shoot length was the distance from the base of the branch to the top bud.

### Experimental methods

*Determination of branch properties.* The initial emergence of 'Cuiguan' shoots in 2023 was on 18 Mar, which was marked as D0 (the start of growth). The full-bloom stage was on 20 Mar 2023 (defined as the beginning of fruit growth; 0 d after full bloom). The number of branches (including vegetative and fruiting shoots) on the test trees and the length and diameter of the newly germinated shoots were recorded. The length was measured by a ruler, and the diameter was measured by electronic digital calipers. Then, the cross-sectional area of the branch-base (CSAB) was calculated according to the equation CSA = $\pi r^2$.

*Determination of fruit quality index.* Healthy trees with uniform growth and no visible signs of disease or pest infestation were selected for each treatment plot, and the treatments were applied in triplicate (a1, a2, and a3) (see Fig. 1A). Fruit samples were collected at various developmental stages, with three representative fruits randomly selected from each tree. Fruit quality indices were determined according to the respective treatment conditions. The 'Cuiguan' fruits without obvious mechanical damage and pests were picked according to the experimental group, and the single fruit weight was determined using an electronic balance (0.001 g). The longitudinal or transverse diameters of the fruits were measured by electronic digital calipers, and the fruit shape index was calculated (fruit shape

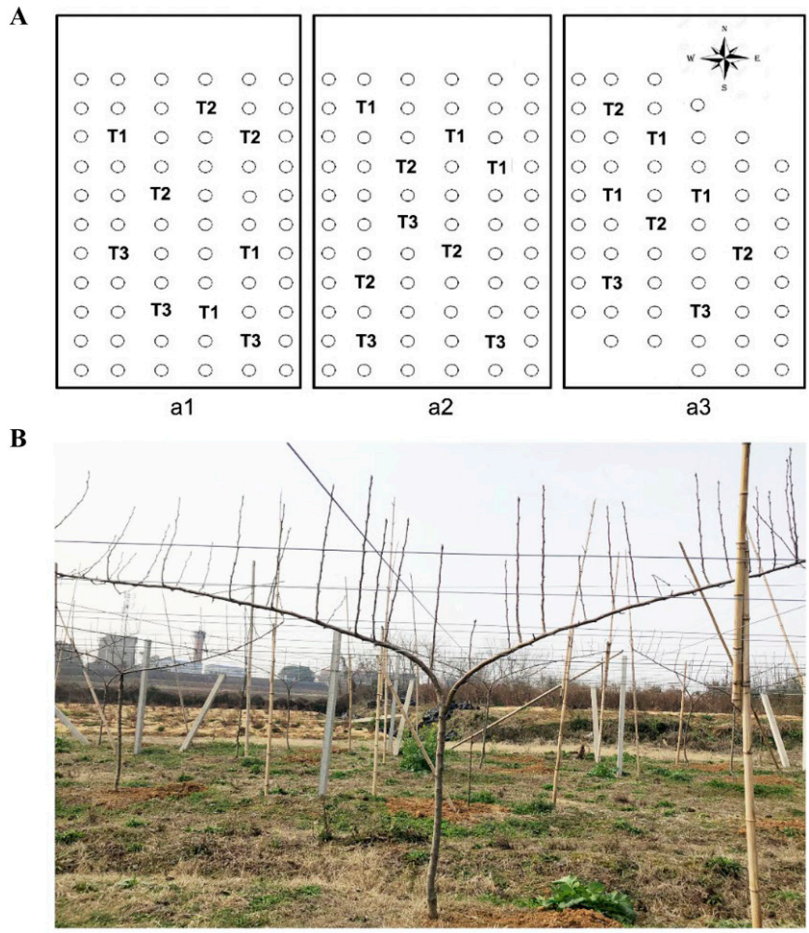


Fig. 1. Diagram of the experimental design (**A**) and the trellised pear trees before branch treatments (**B**). Individual trees were used as experimental units with three replicates in each of the three blocks a1 to a3 in (**A**). T1 (60°), T2 (30°), and T3 (0°) represent different treatments. The tree spacing was 3 m within rows and 4 m between the north-south–oriented rows.

Received for publication 22 Jan 2025. Accepted for publication 2 Jun 2025.
Published online 25 Jul 2025.
This work was financially supported by Grant 2020-620-000-002-05 from the Major Program of Hubei Agricultural Science and Technology Innovation Center, Grant 31801819 from the National Natural Science Foundation of China, and Grant CARS-28 from the China Agriculture Research System. We express our gratitude to EditSprings (https://www.editsprings.cn) for the expert linguistic modification services provided.
L.Y. and T.W.: conceptualization, methodology, software; L.Y. and X.N.: experimental process; L.Y. and Z.L.: data curation, writing–original draft preparation; X.L.: visualization, investigation; H.C.: supervision; Y.C.: management of the experimental orchard and the data validation; F.Y.: writing–reviewing and editing. All authors read and approved the final manuscript.
T.W. is the corresponding author. E-mail: wutaoga556@hbaas.com.

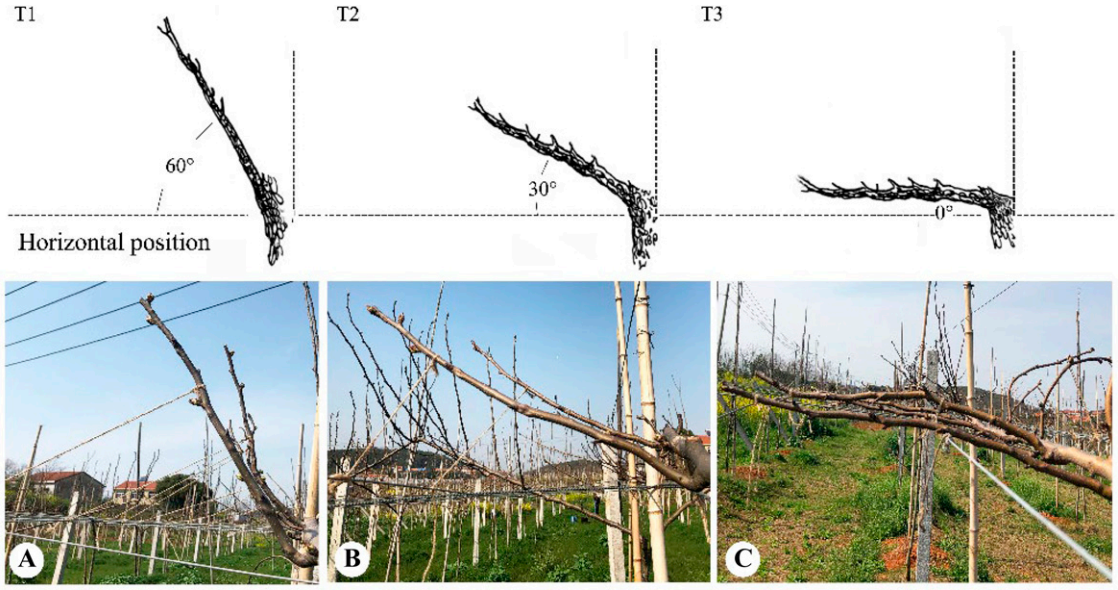


Fig. 2. Schematic diagram of different branch angle treatments on trellised pear trees. (**A**) 60°, (**B**) 30°, and (**C**) 0°.

index = the maximum longitudinal diameter/ the maximum transverse diameter) (Wu et al. 2018). The fruit hardness was measured by a GY-4 digital fruit hardness tester (Zhejiang Topyun Agricultural Science and Technology Co. Ltd., Hangzhou, China). The firmness of the peeled pulp was measured at the fruit's maximum horizontal diameter. Each fruit was measured three times, and the results were averaged. The soluble solids content was determined by a PAL-1 portable digital sugar meter [ATAGO (Aituo) Scientific Instrument Co. Ltd., Tokyo, Japan] (Li et al. 2024). The content of titratable acid was determined by a PAL-Easy portable digital acidity meter [ATAGO (Aituo) Scientific Instrument Co. Ltd.] (Cao et al. 2013). Each sample was measured three times, and the average value was taken.

**Statistical analysis**

Excel 2013 was used for data collation, and the logistic model of branch growth was calculated according to equations reported by Yin (2002). The logistic regression graph of branch length and diameter (as measures of growth) over time was drawn by Origin 9.0 software (with the date as the independent variable and branch length/CSAB as the dependent variable). The values of new shoot growth are calculated according to Eqs. [1] to [6] below. The bar charts of fruit weight, longitudinal and transverse diameters, fresh firmness, and other data were drawn by GraphPad 8 software.

Based on the measured data, including fruit quality determination, shoot length, and CSAB, one-way analysis of variance was performed using SPSS 22.0 software. Pearson's method was used for correlation analysis. The Tukey test was applied to evaluate differences between average values ($P < 0.05$).

Taking the number of days after full bloom as the independent variable and each fruit quality index as the dependent variable, the growth rate equation corresponding to each fruit index was obtained by Wolfram Alpha online derivation. The inflection point was predicted by $-b/2a$ (applicable quadratic equation) and the second derivative $f''(x) = 0$ (applicable cubic equation). The growth processes of branch length and CSAB were modeled using the logistic equation, as presented in Eq. [1]. Eq. [1] was transformed into the linear model $lna + bt = \ln(\frac{k}{y} - 1)$, defined as Eq. [2].

$$y = \frac{k}{1 + ae^{bt}} \quad [1]$$

$$y' = lna + bt = \ln(\frac{k}{y} - 1) \quad [2]$$

The parameters of the model were calculated by linear regression $y' = lna + bt$ and then transformed into the logistic equation. Taking the second derivative of Eq. [1] yields the following expression:

$$\frac{d^2y}{dt^2} = \frac{kab^2e^{bt}(ae^{bt} - 1)}{(1+ae^{bt})^3}.$$

By setting $\frac{d^2y}{dt^2} = 0$, the time of maximum relative growth rate $t_m$ (Eq. [3]) can be obtained:

$$t_m = \frac{lna}{b} \quad [3]$$

Taking the third derivative of Eq. [1] yields:

$$\frac{d^3y}{dt^3} = \frac{kab^3e^{bt}(a^2e^{2bt} - 4ae^{bt} + 1)}{(1+ae^{bt})^4}.$$

By setting $\frac{d^3y}{dt^3} = 0$, the fast growth start time $t_1$ (Eq. [4]) and fast growth end time $t_2$ (Eq. [5]) can be determined:

$$t_1 = \frac{1}{b} ln \frac{2+\sqrt{3}}{a} \quad [4]$$

$$t_2 = \frac{1}{b} ln \frac{2-\sqrt{3}}{a} \quad [5]$$

By taking the first derivative of Eq. [1], the growth rate equation is obtained as follows:

$$v = \frac{dy}{dt} = \frac{-k \cdot abe^{bt}}{(1+ae^{bt})^2} \quad [6]$$

The maximum rate $v_m$ occurs at the extreme point of the derivative. When $m = 1$, the corresponding growth or change rate reaches its maximum, and $v_m$ can be calculated using Eq. [6] as shown in Eq. [7],

$$v_m = \frac{|b|k}{4} \quad [7]$$

where $y$ is the length or thickness of the branch; $t$ is the shoot growth time; $k$ is the theoretical maximum value of shoot length; $a$, $b$ are parameters; $t_1$ is the starting time of rapid shoot growth; $t_2$ is the termination time of rapid shoot growth; $v_m$ is the maximum relative growth rate; $t_m$ is the maximum relative growth time; $t_1$ and $t_2$ are the two points with the fastest rate of daily change, i.e., the time points at which shoot emergence changed to rapid growth and then to slow growth; and $t_2 - t_1$ is the peak growth period.

The $k$ value was determined according to the three-point rule. We took the $t$-equidistant observations $(t_a, y_a)$, $(t_b, y_b)$, and $(t_c, y_c)$ that meet the following conditions:

$$t_b = \frac{t_a + t_c}{2} \quad [8]$$

$$k = \frac{y_b^2(y_a + y_c) - 2y_a y_b y_c}{y_b^2 - y_a y_c} \quad [9]$$

The growth period was separated into the early growth stage ($t = 0$ to $\frac{lna-1.317}{b}$), d; rapid growth stage ($t = \frac{lna-1.317}{b}$ to $\frac{lna+1.317}{b}$), d; and late growth stage ($t = \frac{lna+1.317}{b}$ to later), d. According to the values of $k$ and $y$, a series of $y'$

values corresponding to different time points were obtained. Then, the linear regression equation was fitted with time as the independent variable and $y'$ as the dependent variable, and the $R^2$ value was obtained.

## Results and Analysis

### Construction of new shoot length and CSAB growth model under different branch-base angle treatments

The time-course changes in the new shoot length and diameter of trellised pear can be characterized by Eq. [1] (Fig. 3). The growth of new shoots showed an S-shaped trend over time regardless of the treatment. The results on the proportion of branch types indicated that branch-angle treatments significantly affected shoot vegetative development. When the horizontal angle of branches approached 0°, the proportion of short shoots increased significantly ($P < 0.05$), while the proportion of medium-length shoots decreased correspondingly. However, no statistically significant difference was observed in the proportion of long shoots among the three treatments ($P > 0.05$) (Table 1).

The correlation coefficients of the relationships shown in Fig. 3 were more than 0.9, indicating high significance; moreover, the theoretical maximum value $k$ was very close to the measured value (Table 2). Therefore, the constructed logistic model provided a relatively reliable prediction of the growth of new shoots during the period monitored.

Total shoot numbers were recorded on experimental branches subjected to different branch angle treatments at the end of the growing period (mid-Jul 2023). The data are presented as means ± standard error (*SE*) ($n = 3$, representing three replicate plots). Different letters within the same column indicate statistically significant differences among treatments ($P < 0.05$).

### Stages of new shoot growth under different branch-base angle treatments

The shoot growth rate was assessed using Eqs. [3] to [6] (Table 3). The growth of new shoots (length and CSAB) can be divided into three stages: early growth stage $(0, t_1)$, rapid growth stage $(t_1, t_2)$, and late growth stage $(t_2, t_n)$ (Table 4). The results showed that in terms of elongation growth, although the T1 group entered the rapid growth period about 2 d later (16th April) compared with T2 and T3, there was no significant difference in the duration of the initial growth period and the rapid growth period among the three treatments. In addition, there was no significant difference in the maximum growth rate $v_m$ (at $\alpha = 0.05$). In terms of CSAB, in the T3 group, the termination of rapid growth ($t_2$) was significantly ($P < 0.05$) earlier, and the duration of the rapid growth period was significantly shorter than in the T1 and T2 groups.

Under different treatments, with the decrease of branch-base angle, the rapid shoot elongation growth ($t_1$) gradually started earlier (Table 3). On the contrary, the starting time of rapid shoot thickening (i.e., increased CSAB) was gradually delayed from T1 to T3. In terms of CSAB growth, the maximum growth time ($t_m$) was nearly a week earlier (6.14 d) in T3 than in T1, and the maximum relative growth rate $v_m$ of T3 was about 2.02 times greater than in T1. There were no significant differences (at $\alpha = 0.05$) in the maximum growth time and the maximum relative growth rate regarding shoot length growth.

$t_1$ is the starting time of rapid growth; $t_2$ is the termination time of rapid growth; $v_m$ is the maximum relative growth rate; and $t_m$ is the maximum growth time. The values are means ± *SE* ($n = 3$). For specific measurements, different letters in each column indicate significant differences among treatments ($P < 0.05$).

### Time-course changes in length and CSAB of new shoots in different branch-base angle treatments

The two main branches of the "double-arm" trellised pear trees extend in the north−south direction, with symmetrical distribution of branches. The growth rate of shoots on the main branches determines the expansion of its crown width. Table 5 showed that in the early stage of growth, there was no significant treatment difference in the average shoot elongation rate (at $\alpha = 0.05$), but the average growth rate of CSAB was significantly higher in T3 than in T1 and T2.

During the rapid growth period, the average shoot elongation rate decreased in the order T2 > T1 > T3, and there was a significant difference between T2 and T3 ($P < 0.05$). The average growth rate of CSAB was significantly higher in T3 than in T1 and T2, which was similar to that in the early stage of growth.

At the late growth stage, the average shoot elongation rate was T2 > T1 > T3, and there was a significant difference between T2 and T3 ($P < 0.05$). The average growth rate of CSAB decreased in the order T3 > T2 > T1, with significant differences among the three groups ($P < 0.05$). In general, in terms of the shoot elongation rate, the difference between T1 and T3 groups was not obvious in the three periods, and the average shoot elongation rate of T2 was relatively high in the rapid growth and the late growth stages. In terms of CSAB growth rate, the T3 group was significantly faster than the T1 and T2 groups, especially in the late growth stage.

### Construction of mathematical model of fruit growth under different branch-base angles

We measured three growth indices (longitudinal diameter, transverse diameter, and weight) and two indicators of fruit ripening (total soluble solid content and fresh firmness) during fruit growth (78 to 127 d after full bloom) under three different branch-base angle treatments and fitted the appropriate time-course curves. The corresponding fitting curves and derivative function diagrams are shown in Table 6.

The quadratic equation was used to fit the four indices of fruit quality (weight, total soluble solid content, transverse diameter, and longitudinal diameter), whereas the cubic

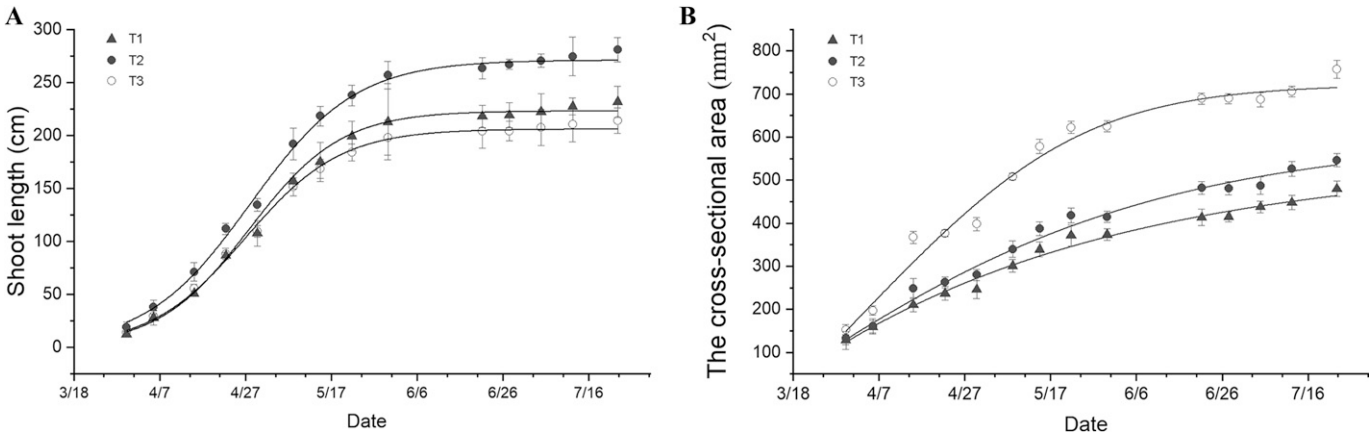


Fig. 3. The fitted curves of average length (**A**) and cross-sectional area of branch base (**B**) of new shoots developed on treated branches of trellised 'Cuiguan' pear trees. T1 = 60° branch-base angle, T2 = 30° branch-base angle, T3 = 0° branch-base angle. Each point represents the average value ($n = 3$, three repeated experimental plots).

Table 1. Proportion of shoot types (short, medium, and long) in response to three branch-angle treatments in 'Cuiguan' trellised pear trees cultivated in Wuhan, China.

| | Total number | | | | | |
|---|---|---|---|---|---|---|
| Treatment | Short shoots (≤50 cm) | Medium shoots (>50 to ≤100 cm) | Long shoots (>100 cm) | Short shoots (%) | Medium shoots (%) | Long shoots (%) |
| T1 | 425 | 144 | 13 | 73.01 ± 0.70 b | 24.78 ± 1.74 a | 2.21 ± 1.52 a |
| T2 | 541 | 159 | 24 | 74.83 ± 2.10 b | 21.99 ± 2.30 ab | 3.18 ± 0.23 a |
| T3 | 480 | 117 | 18 | 78.84 ± 1.50 a | 19.21 ± 2.15 b | 1.96 ± 0.78 a |

Table 2. Logistic model parameters and the test indices of average growth of shoot length and cross-sectional area of branch base (CSAB) on 1-year-old branches of trellised pear trees.

| Measurement | Treatment | Logistic equation | Correlation coefficient $r$ | Coefficient of Determination $R^2$ | Theoretical value $k$ | Measured value $k$ |
|---|---|---|---|---|---|---|
| Length (cm) | T1 | $y = 231.78/(1 + 26.66e^{-0.0692t})$ | 0.96 | 0.93 | 232 | 232 |
| | T2 | $y = 280.91/(1 + 21.37e^{-0.0665t})$ | 0.97 | 0.94 | 281 | 281 |
| | T3 | $y = 214.07/(1 + 22.15e^{-0.0688t})$ | 0.97 | 0.94 | 214 | 214 |
| CSAB ($mm^2$) | T1 | $y = 478.54/(1 + 5.79e^{-0.0354t})$ | 0.99 | 0.97 | 479 | 456 |
| | T2 | $y = 552.84/(1 + 6.44e^{-0.0376t})$ | 0.98 | 0.97 | 553 | 527 |
| | T3 | $y = 745.72/(1 + 7.35e^{-0.0459t})$ | 0.96 | 0.93 | 746 | 738 |

Table 3. Growth parameters of shoot length and cross-sectional area of branch base (CSAB).

| Measurement | Treatment | $t_1$ (d) | $t_2$ (d) | $t_2 - t_1$ (d) | $t_m$ (d) | $v_m$ (cm/d, $mm^2$/d) |
|---|---|---|---|---|---|---|
| Length (cm) | T1 | 28.41 ± 3.19 a | 66.47 ± 1.70 a | 38.06 ± 3.10 a | 47.44 ± 8.12 a | 4.01 ± 0.15 a |
| | T2 | 26.24 ± 2.17 a | 65.85 ± 0.99 a | 39.61 ± 3.04 a | 46.05 ± 5.88 a | 4.67 ± 0.65 a |
| | T3 | 25.88 ± 2.63 a | 64.17 ± 3.96 a | 38.28 ± 1.97 a | 45.03 ± 5.64 a | 3.68 ± 0.39 a |
| CSAB ($mm^2$) | T1 | 12.41 ± 1.80 a | 86.82 ± 6.93 a | 74.4 ± 4.76 a | 49.61 ± 3.45 a | 4.24 ± 0.52 b |
| | T2 | 14.53 ± 1.26 a | 84.58 ± 0.74 a | 70.05 ± 1.31 a | 49.55 ± 1.39 a | 5.20 ± 0.67 b |
| | T3 | 14.78 ± 1.78 a | 72.16 ± 3.15 b | 57.38 ± 5.79 b | 43.47 ± 1.99 b | 8.56 ± 1.54 a |

Table 4. Duration of developmental stages (in days) regarding the shoot length and cross-sectional area of branch base (CSAB) growth.

| Measurement | Treatment | Early growth stage | Rapid growth stage | Late growth stage |
|---|---|---|---|---|
| Length (cm) | T1 | 18 Mar to about 15 Apr | About 16 Apr to 24 May | From 25 May onward |
| | T2 | 18 Mar to about 13 Apr | About 14 Apr to 24 May | From 25 May to onward |
| | T3 | 18 Mar to about 13 Apr | About 14 Apr to 22 May | From 23 May to onward |
| CSAB ($mm^2$) | T1 | 18 Mar to about 30 Mar | About 31 Mar to 13 Jun | From 14 Jun to onward |
| | T2 | 18 Mar to about 2 Apr | About 3 Apr to 11 Jun | From 12 Jun to onward |
| | T3 | 18 Mar to about 2 Apr | About 3 Apr to 31 May | From 1 Jun to onward |

The starting date was 18 Mar.

equation fitted the remaining index (flesh firmness). Over time, in all treatments, the fruit transverse and longitudinal diameter and fruit weight showed an increasing trend, while the daily growth rate showed a decreasing trend (Figs. 4–6). The relative treatment differences in the daily growth rate of these three indicators appeared only after about 95 to 105 d after full bloom (Figs. 4B–6B).

For total soluble solid content, the fitted curves were similar for T1 and T2. By contrast, the daily growth rate was lower in T3 than T1 and T2 in the early stage, but the reverse was obvious in the late growth stage (Fig. 7). The growth curve of flesh firmness under T2 and T3 treatments was fitted with a cubic equation, indicating that the trend of fruit flesh texture development was subject to more complex influences from branch bending angles (Fig. 8).

### Comparison of quality characteristics of mature fruits under different branch-base angle treatments

According to the results (Fig. 9), there was no significant difference (at $\alpha = 0.05$) in single fruit weight, fruit shape index, transverse and longitudinal diameters, and soluble sugar content across the three branch-pulling angles. The average content of titratable acid in T1 group was significantly higher than that in T2 and T3 groups ($P < 0.05$), but there was no difference between T2 and T3. In terms of solid-to-acid ratio, T3 group was significantly ($P < 0.05$) higher than T1 group but not significantly different from T2. Regarding the flesh firmness of the 'Cuiguan' fruit, it was significantly ($P < 0.05$) lower in the T2 and T3 treatments than in T1. Taking into account all the fruit quality indices, the quality of the 'Cuiguan' fruit was better in T3 than in T1 and T2 groups.

## Discussion

### Branch-base angle trainings significantly altered the vegetative growth patterns in new formed shoots

The results demonstrated that branch bending angles had a significant impact on the proportion of short shoots in pear trees. This observation aligns with the reported physiological mechanism whereby horizontal branch orientation disrupts auxin transport, thereby weakening apical dominance and promoting lateral bud development (Balla et al. 2016). Our findings are consistent with those from 'Pingguo' pear orchards, where vertical bending at 80° to 90° (i.e., a horizontal angle of 0° to 10°) significantly increased the formation of medium and short shoots compared with 60° and 120° angles (Wu et al. 2008). However, they contrast with results from high-density apple orchards, where a vertical angle of 110° (i.e., a horizontal angle of −20°) resulted in the highest proportion of medium and short shoots compared with 70°, 90°, and 130° (Gao et al. 2022). This divergence suggests species-specific sensitivity to branch-angle manipulation. Furthermore, planting density may also contribute to these differences. In low-density orchards, a horizontal branch angle of 0° may optimize vegetative growth and fruiting efficiency, whereas in high-density systems, this configuration may

Table 5. Comparison of average growth rates of shoot length and cross-sectional area of branch base (CSAB).

| Measurement | Treatment | Early growth stage | Rapid growth stage | Late growth stage |
|---|---|---|---|---|
| Length (cm/d) | 60° (T1) | 1.72 ± 0.24 a | 3.52 ± 0.25 ab | 3.37 ± 0.54 ab |
| | 30° (T2) | 2.26 ± 0.32 a | 4.09 ± 0.38 a | 4.05 ± 0.14 a |
| | 0° (T3) | 1.75 ± 0.22 a | 3.23 ± 0.20 b | 3.02 ± 0.13 b |
| CSAB ($mm^2$/d) | 60° (T1) | 8.15 ± 0.25 b | 3.71 ± 0.25 b | 9.47 ± 0.34 c |
| | 30° (T2) | 8.05 ± 0.10 b | 4.56 ± 0.20 b | 10.54 ± 0.33 b |
| | 0° (T3) | 10.67 ± 0.44 a | 7.5 ± 0.58 a | 11.69 ± 0.46 a |

The values are means ± standard error (n = 30 to 45 branches/treatment). For a given measurement, different letters in each column indicate significant differences among treatments ($P < 0.05$).

Table 6. Curve fitting equations of the main indicators constructed based on the days of fruit development.

| Classification | Treatment | Equation of fitting curve | Coefficient $R^2$ of determination | $P$ value |
|---|---|---|---|---|
| Weight | T1 | $y1 = -542.28 + 9.38x + -0.017x^2$ | 1.00 | $P < 0.01$ |
| | T2 | $y2 = -682.63 + 11.82x + -0.03x^2$ | 0.99 | $P < 0.01$ |
| | T3 | $y3 = -1006.31 + 18.21x + -0.06x^2$ | 0.97 | $P < 0.01$ |
| Total soluble solid | T1 | $y1 = 1.20 + 0.14x + -0.0004x^2$ | 0.98 | $P < 0.01$ |
| | T2 | $y2 = 0.69 + 0.12x + -0.0002x^2$ | 0.98 | $P < 0.01$ |
| | T3 | $y3 = 8.46 + -0.004x + 0.0003x^2$ | 0.99 | $P < 0.01$ |
| Transverse diameter | T1 | $y1 = -87.56 + 2.47x + -0.009x^2$ | 0.98 | $P < 0.01$ |
| | T2 | $y2 = -79.82 + 2.35x + -0.008x^2$ | 0.99 | $P < 0.01$ |
| | T3 | $y3 = -109.78 + 2.9688x - 0.0111x^2$ | 0.99 | $P < 0.01$ |
| Longitudinal diameter | T1 | $y1 = -60.04 + 1.92x + -0.006x^2$ | 1.00 | $P < 0.01$ |
| | T2 | $y2 = -98.81 + 2.73x + -0.0102x^2$ | 1.00 | $P < 0.01$ |
| | T3 | $y3 = -74.71 + 2.21x + -0.0076x^2$ | 0.97 | $P < 0.01$ |
| Flesh firmness | T1 | $y1 = 54.28 + -0.79x + 0.003x^2$ | 0.92 | $P < 0.01$ |
| | T2 | $y2 = 16.66 + -0.07x - 9.44e^{-007}x^3$ | 0.88 | $P = 0.04$ |
| | T3 | $y3 = 31.98 + -0.29x + 5.17e^{-006}x^3$ | 1.00 | $P < 0.01$ |

not be optimal for maintaining tree vigor and economic productivity.

### Branch-base angle greatly affected the CSAB and length growth of the new shoots of the trellised pear trees

In general, the smaller the horizontal angle of branches, the smaller the growth of branch length, making it more conducive to the transformation from vegetative growth to reproductive growth. In this study, the three branch-base angle treatments [60° (T1), 30° (T2), and 0° (T3)] all resulted in rapid growth of new shoots from mid-April to mid-to-late May, which slowed down after early June (Fig. 3A); these findings were consistent with the trend of new shoots growth of 'Huangguo' pear trees under natural conditions (Liu et al. 2020). There was almost no CSA growth peak in T1 and T2 treatment groups (Fig. 3A), and the average length of new shoot growth in T2 (30°) group was the longest, followed by T1 (60°) and T3 (0°) (Fig. 3B). These findings contradict the results reported by Wu et al. (2008) for 'Pingguo' pear trees, in which branch average length decreased with increasing stretching angles of 50° to 60° (the horizontal angle is ~30° to 40°), 80° to 90° (the horizontal angle is ~0° to 10°), and 120° (the horizontal angle is about −30°), showing a consistent pattern. The discrepancy may be attributed to differences in varieties and cultivation practices.

Specifically, in terms of elongation growth, the vegetative growth of shoots in the T3 group was most inhibited, and the average length of new shoots was consistently shorter than that in the T1 and T2 groups (Fig. 3A). Regarding CSAB growth, compared with the T1 and T2 treatment groups, the maximum relative growth rate $v_m$ of branches in the T3 group was significantly higher ($P < 0.05$) (Table 3), and the rapid growth period was shortened by 11 to 16 d (Table 4). This may be related to the carbon transport capacity of short branches being greater than that of long branches (Rosati et al. 2018; Sansavini and Corelli 1992). Under such conditions, the T3 group entered a period of slow CSAB growth 11 d earlier than the T2 group and 13 d earlier than the T1 group.

### Different branch angles influenced the fruit quality formation on trellised 'Cuiguan' pear

The results of this study confirmed that the regulation mechanism of pear fruit quality under different branch angles may be closely related to the growth rhythm of the branches. Wei et al. (2018) carried out branch pulling experiments at different angles on Korla fragrant pear trees in spindle-shaped close planting mode. Contrary to the present study on 'Cuiguan' pear, the content of soluble solids and the sugar-to-acid ratio in Korla fragrant pear significantly increased at a vertical angle of approximately 75°, whereas flesh firmness decreased and titratable acid content remained unchanged. These differences may be attributed to variations in fruit cultivars or the spatial distribution of endogenous hormones under different angles. Branch angle not only affects the transport pathway of photosynthetic products but also alters the distribution of endogenous hormones through mechanical stress

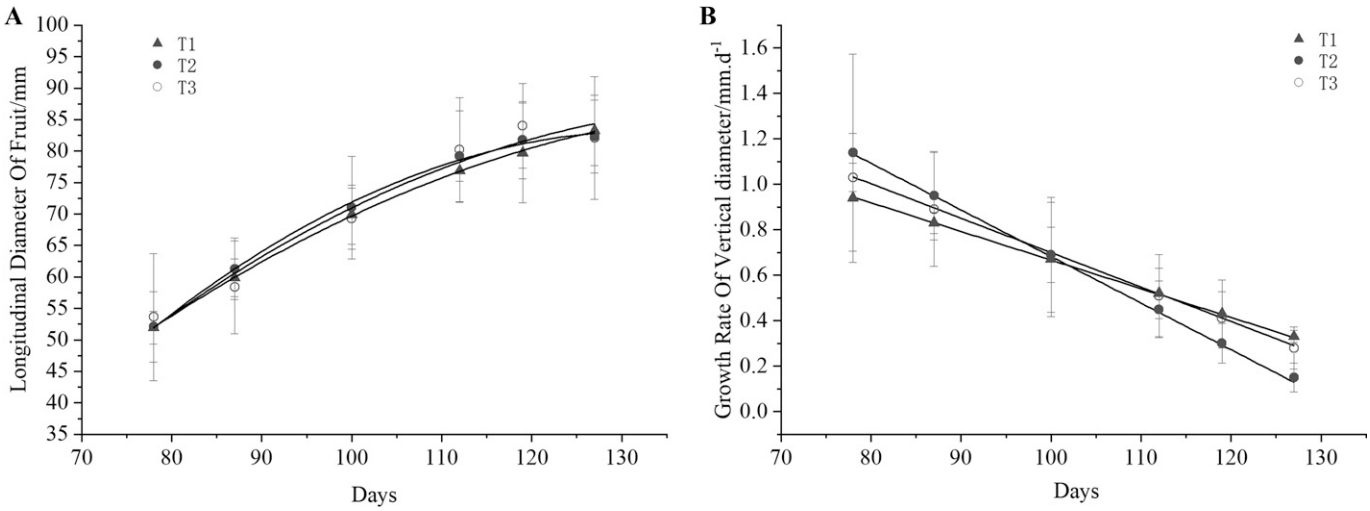


Fig. 4. Time-course changes in the fruit longitudinal diameter of 'Cuiguan' pear under different branch-base angle treatments. (**A**) Longitudinal diameter of fruit. (**B**) Growth rate of vertical diameter. T1 = 60° branch-base angle, T2 = 30° branch-base angle, T3 = 0° branch-base angle. Each point represents the mean ± standard error of fruit growth measurements ($n = 3$, three repeated experimental plots).

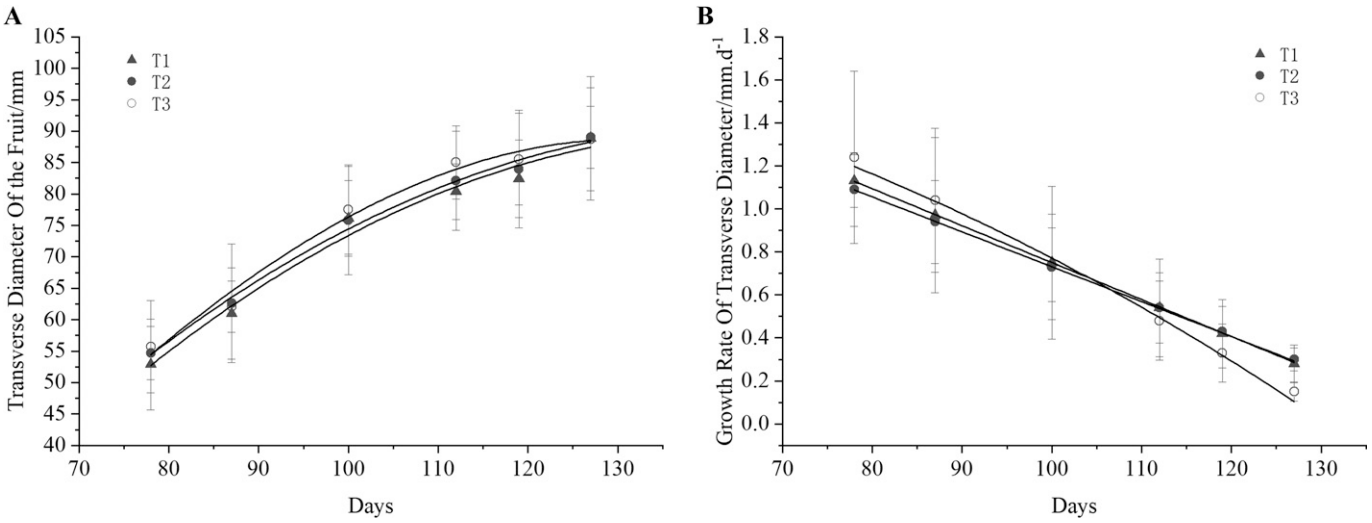


Fig. 5. Time-course changes in the transverse diameter of 'Cuiguan' pear under different branch-base angle treatments. (**A**) Transverse diameter of fruit. (**B**) Growth rate of transverse diameter. T1 = 60° branch-base angle, T2 = 30° branch-base angle, T3 = 0° branch-base angle. Each point represents the mean ± standard error of fruit growth measurements ($n$ = 3, three repeated experimental plots).

signals, thereby influencing plant growth and productivity (Reis et al. 2018). This creates conditions that inhibit vegetative growth while promoting fruit ripening and the formation of sugar and acid content (Batista-Silva et al. 2018; He et al. 2005). From the analysis of shoot growth dynamics, the T3 group ended its rapid growth stage earlier than the T1 and T2 groups (Table 4) and exhibited a significantly faster growth rate.

This adjustment of growth rhythm may affect fruit development through two aspects. First, the early cessation of shoot growth reduces nutrient competition with fruit development, allowing more carbon assimilates to be allocated to the fruit and accelerating the conversion of organic acids to carbohydrates in pulp cells, thereby improving the sugar-to-acid ratio (Fig. 9G). Second, the T3 group showed a stronger inhibitory effect on apical growth, which greatly promoted lateral branch development, improved the overall growth rate, and accelerated the expression of genes related to fruit ripening, resulting in decreased flesh firmness (Fig. 9H). In addition, through the determination of fruit quality parameters for 4 consecutive months, it was found that the three branch angle treatments did not influence the overall trend of daily growth rate of fruit longitudinal and transverse diameters and weight, which all decreased during fruit development. However, for fruit and flesh firmness, the T3 and T2 groups showed an increasing (rather than decreasing) trend (Figs. 7B and 8B). Overall, it was found that 95 to 110 d after full bloom was an important period resulting in changes in the relative daily growth rate of the above five quality parameters, while the branches achieved more than 90% of the annual growth in this period (Fig. 3), just before the late growth stage. Therefore, coordinating and enhancing the nutritional management of shoots and fruits before this period (mid-to-late June) may be important to both ensuring optimal fruit quality and stabilizing tree vigor.

## Conclusions

Different branch-base angles of trellised pear trees influenced the growth rate of new shoots and the fruit quality parameters (titratable acid, flesh firmness, and solid-to-acid ratio). Before mid-to-late June is an important period for the implementation of interventions to balance the nutritional management of shoots and fruits. The curve-fitting equations and functions of 'Cuiguan' shoots and fruits grown in the "Double Primary Branches along the Row" orchard with the flat-type trellis system cultivation mode can accurately reflect the growth dynamics of branches and predict the key growth periods. It provides a basis for accurately and quantitatively studying the dynamic changes in branch growth and nutrient regulation and also provides important

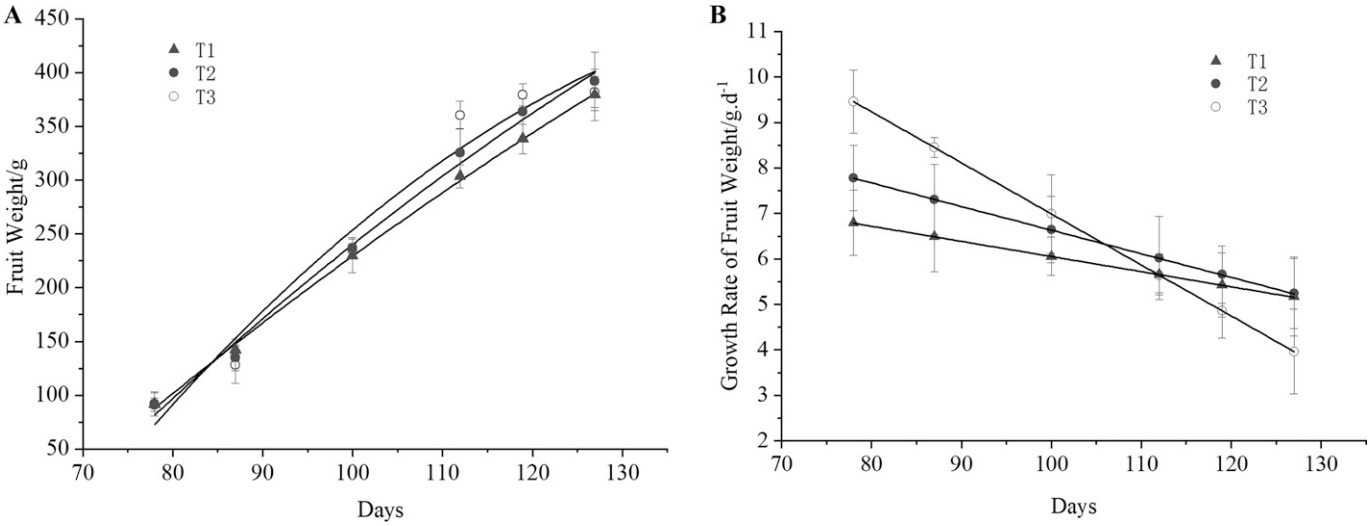


Fig. 6. Time-course changes in the weight of 'Cuiguan' pear fruits under different branch-base angle treatments. (**A**) Fruit weight. (**B**) Growth rate of fruit weight. T1 = 60° branch-base angle, T2 = 30° branch-base angle, T3 = 0° branch-base angle. Each point represents the mean ± standard error of fruit growth measurements ($n$ = 3, three repeated experimental plots).

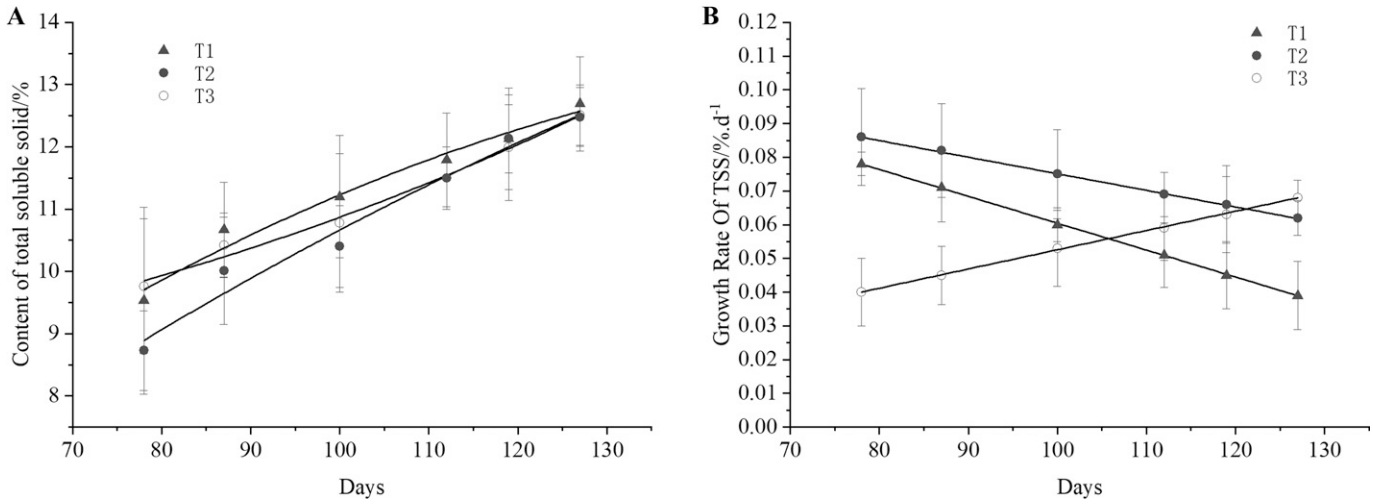


Fig. 7. Time-course changes in the total soluble solids (TSS) content of 'Cuiguan' pear fruits under different branch-base angle treatments. (**A**) Content of TSS. (**B**) Growth rate of TSS. T1 = 60° branch-base angle, T2 = 30° branch-base angle, T3 = 0° branch-base angle. Each point represents the mean ± standard error of fruit growth measurements ($n$ = 3, three repeated experimental plots).

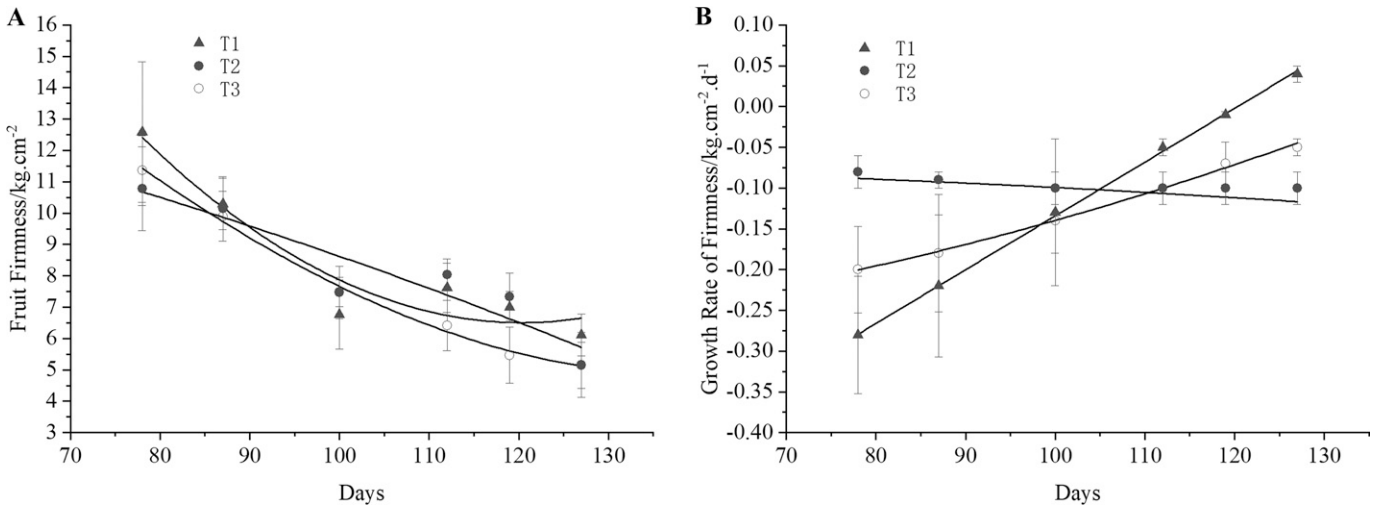


Fig. 8. Time-course changes in fruit flesh firmness of 'Cuiguan' pear under different branch-base angle treatments. (**A**) Fruit firmness. (**B**) Growth rate of firmness. T1 = 60° branch-base angle, T2 = 30° branch-base angle, T3 = 0° branch-base angle. Each point represents the mean ± standard error of fruit growth measurements ($n$ = 3, three repeated experimental plots).

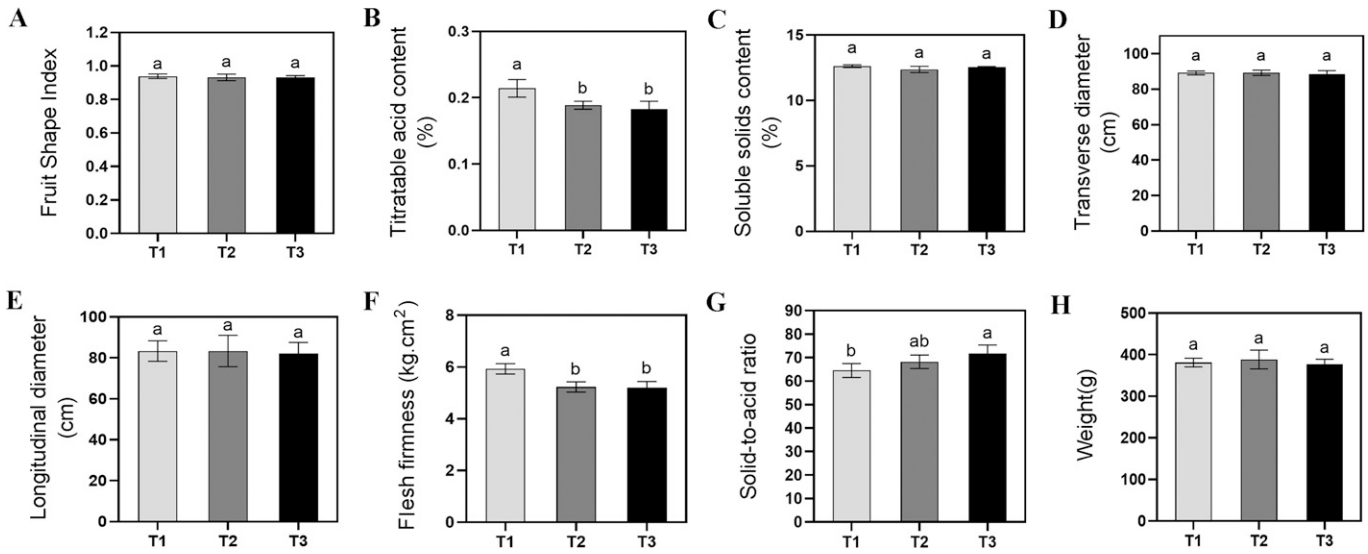


Fig. 9. The effects of different branch base angle treatments on various quality parameters of mature 'Cuiguan' pear fruits. (**A**) Fruit shape index. (**B**) Titratable acid content. (**C**) Soluble solids content. (**D**) Transverse diameter. (**E**) Longitudinal diameter. (**F**) Flesh firmness. (**G**) Solid-to-acid ratio. (**H**) Weight. T1 = 60° branch-base angle, T2 = 30° branch-base angle, T3 = 0° branch-base angle. Bars indicate the means of fruit growth measurements ± standard error ($n$ = 3, three repeated experimental plots). Different letters indicate statistically significant differences at the $P$ = 0.05 level.

support for predicting the quality changes of pear fruit under different management conditions. It can provide a theoretical reference for optimizing the management of trellised pear trees in production.

### References Cited


Balla J, Medved'ová Z, Kalousek P, Matiješčuková N, Friml J, Reinöhl V, Procházka S. 2016. Auxin flow-mediated competition between axillary buds to restore apical dominance. Sci Rep. 6:35955. https://doi.org/10.1038/srep35955.

Bao D, Liu Z, Song L. 2007. Study on mathematical model of fruit growth and development of Jintaiyang apricot. Anhui Agric Sci. 35(4):945–946. https://doi.org/10.3969/j.issn.0517-6611.2007.04.002.

Batista-Silva W, Nascimento VL, Medeiros DB, Nunes-Nesi A, Ribeiro DM, Zsögön A, Araújo WL. 2018. Modifications in organic acid profiles during fruit development and ripening: Correlation or causation? Front Plant Sci. 9:1689. https://doi.org/10.3389/fpls.2018.01689.

Cai X, Pan J, Zhou Y, Liu H, Huang G. 2016. Study on the mathematical model of fruit growth and development of Taiwan pineapple Sakya. Anhui Agric Sci. 44:44–45, 96. https://doi.org/10.3969/j.issn.0517-6611.2016.27.015.

Cao J, Jiang W, Zhao Y. 2013. Guidance of postharvest physiological and biochemical experiments of fruits and vegetables. China Light Industry Press, Beijing, China.

Dai ZW, Génard M, Li S, Vivin P. 2009. Analyzing the functional association among seed traits, berry growth and chemical composition in Cabernet-Sauvignon berry (*Vitis vinifera* L.) using a mathematical growth function. J Int Sci Vigne Vin. 43:35–44. https://doi.org/10.20870/oeno-one.2009.43.1.807.

Gao J, Wang Q, Cai H, Li C, Du X, Wang S, Yang T. 2022. Effects of branch bending angle on tree growth and fruit production of 'Nagafu No. 2' apple grafted on SH1 dwarfing interstock. China Fruit Trees. 11:56–58. https://doi.org/10.16626/j.cnki.issn1000-8047.2022.11.011.

Genard M, Reich M, Lobit P, Besset J.1999. Correlations between sugar and acid content and peach growth. J Hortic Sci Biotechnol. 74(6):772–776. https://doi.org/10.1080/14620316.1999.11511187.

Han S, Luo L, Lu J, He E, Lu Z. 2023. Fruit development dynamics and model establishment of macadamia in Guizhou. Seeds. 42: 79–85 + 97. https://doi.org/10.16590/j.cnki.1001-4705.2023.04.079.

He Z, Li W, Lin X, Pan W, Su D, Zhuang L. 2005. Metabolism of organic acids during loquat fruit ripening and storage. J Pomol. 22:23–26. https://doi.org/10.3969/j.issn.1009-9980.2005.01.006.

Hillmann L, Elsysy M, Goeckeritz C, Hollender C, Rothwell N, Blanke M, Einhorn T. 2021. Preanthesis changes in freeze resistance, relative water content, and ovary growth preempt bud phenology and signify dormancy release of sour cherry floral buds. Planta. 254(4):74. https://doi.org/10.1007/s00425-021-03722-0.

Jung SK, Choi HS. 2010. Light penetration, growth, and fruit productivity in 'Fuji' apple trees trained to four growing systems. Sci Hortic. 125(4):672–678. https://doi.org/10.1016/j.scienta.2010.05.027.

Jung SK, Ryu HU, Gu M, Choi HS, Ryu JH, Cho YK. 2012. Growth and fruit production in young 'Fuji' apple trees as affected by time of downward bending of branches. J Hortic Sci Biotechnol. 87(5):519–523. https://doi.org/10.1080/14620316.2012.11512905.

Lauri PÉ, Lespinasse JM. 2001. Genotype of apple trees affects growth and fruiting responses to shoot bending at various times of year. J Am Soc Hortic Sci. 126(2):169–174. https://doi.org/10.21273/JASHS.126.2.169.

Li S, Zhou Q, Hao X, Zhang T, Hao Y, Jiang Y, Lu Y. 2024. Effects of different thickness of plastic film packaging on storage quality of plum fruit. China Fruit Trees. 5:45–51. https://doi.org/10.16626/j.cnki.issn1000-8047.2024.05.007.

Liu X, Gu W, Wei H, Shi W, Liao D. 2020. 'Huangguo' growth rhythm and regression analysis of fitting curve. Northern Hortic. 18:1–6. https://doi.org/10.11937/bfyy.20194703.

Ma HL, Chen GQ, Qiang J. 2019. Preliminary study on the effects of branch angle and branch height on disease and sunburn of precocious walnut fruit. Northern Hortic. 21:20–24. https://doi.org/10.11937/bfyy.20191011.

Musacchi S, Iglesias I, Neri D. 2021. Training systems and sustainable orchard management for European pear (*Pyrus communis* L.) in the Mediterranean area: A review. Agronomy. 11(9):1765. https://doi.org/10.3390/agronomy11091765.

Panghal P, Kumar M, Rani S. 2019. Estimation of annual compound growth rates of guava (*Psidium guajava* L.) fruit in Haryana using non linear model. J Appl Nat Sci. 11(4):778–784. https://doi.org/10.31018/jans.v11i4.2175.

Panta S, Zhou B, Zhu L, Maness N, Rohla C, Costa L, Ampatzidis Y, Fontainer C, Kaur A, Zhang L. 2023. Selecting non-linear mixed effect model for growth and development of pecan nut. Sci Hortic. 309:111614. https://doi.org/10.1016/j.scienta.2022.111614.

Peng J, Pan J, Wu Y, He J, Deng Y, Xu J, Duan C, Liu Y. 2021. Research on flowering habits and fruit growth model of Guifeng early longan. J Fruit Sci. 38:947–956. https://doi.org/10.13925/j.cnki.gsxb.20200555.

Qi P, Zhang L, Wang Z, Han H, Müller J, Li T, Wang C, Huang Z, He M, Liu Y, He X. 2023. Effect of operational parameters of unmanned aerial vehicle (UAV) on droplet deposition in trellised pear orchard. Drones. 7(1):57. https://doi.org/10.3390/drones7010057.

Qin L, Wu Y, Shi H. 2011. Effects of branch bending phases and angles on the branch growth of apple with dwarfing intermediate stock. Hebei Agric Sci. 15:13–15. https://doi.org/10.3969/j.issn.1088-1631.2011.04.00.

Reis GSM, Almeida AAFD, Mangabeira PAO, Santos ICD, Pirovani CP, Ahnert D. 2018. Mechanical stress caused by wind on leaves of *Theobroma cacao*: Photosynthetic, molecular, antioxidative and ultrastructural responses. PLoS One. 13(6):e0198274. https://doi.org/10.1371/journal.pone.0198274.

Rizzolo A, Vanoli M, Torricelli A, Spinelli L, Sadar N, Zanella A. 2021. Modeling optical properties of 'Braeburn' apples during fruit maturation on the tree. Acta Hortic. 1311: 113–122. https://doi.org/10.17660/ActaHortic.2021.1311.15.

Rosati A, Paoletti A, Al Hariri R, Famiani F. 2018. Fruit production and branching density affect shoot and whole-tree wood to leaf biomass ratio in olive. Tree Physiol. 38(9): 1278–1285. https://doi.org/10.1093/treephys/tpy009.

Samant D, Kishore K, ICAR-IIHR-Central Horticultural Experiment Station, Bhubaneswar-751 019, India 2021. Response of guava var. Arka Amulya to branch bending during winter and summer in the Eastern tropical region of India. J Environ Biol. 42(3):720–726. https://doi.org/10.22438/jeb/42/3/MRN-1581.

Sansavini S, Ancarani V, Neri D. 2008. Overview of intensive pear culture: Planting density, rootstocks, orchard management, soil-water relations and fruit quality. X Int Pear Symp 800. 2007:35–50. https://doi.org/10.17660/ActaHortic.2008.800.1.

Sansavini S, Corelli L. 1992. Canopy efficiency of apple as affected by microclimatic factors and tree structure. Acta Hortic. 322:69–78. https://doi.org/10.17660/ActaHortic.1992.322.7.

Tudela V, Santibáñez F. 2016. Modelling impact of freezing temperatures on reproductive organs of deciduous fruit trees. Agric For Meteorol. 226–227:28–36. https://doi.org/10.1016/j.agrformet.2016.05.002.

Wei J, Jiang Y, Ma J, Shi L. 2018. Effects of branch angle on branch and leaf growth and fruit quality of Korla fragrant pear. J Northwest For Univ. 33:111–116. https://doi.org/10.3969/j.issn.1001-7461.2018.03.17.

Wu S, Zhang B, Keyhaninejad N, Rodríguez GR, Kim HJ, Chakrabarti M, Illa-Berenguer E, Taitano NK, Gonzalo MJ, Díaz A, Pan Y, Leisner CP, Halterman D, Buell CR, Weng Y, Jansky SH, Van Eck H, Willemsen J, Monforte AJ, Meulia T, Van Der Knaap E. 2018. A common genetic mechanism underlies morphological diversity in fruits and other plant organs. Nat Commun. 9(1):4734. https://doi.org/10.1038/s41467-018-07216-8.

Wu T, Qin Z, Yang F, Tu J, Li X, Zhu H. 2015. 'Double-arm forward' new trellis pruning technique for pear trees. Southern China Fruit Trees. 44:133–134. https://doi.org/10.13938/j.issn.1007-1431.20150255.

Wu T, Qin Z, Yang F, Zhu H, Li X. 2014. A new type of trellis pear tree shape and its shaping method. CN103081770B. 12 March 2014.

Wu X, He Z, Yang Y. 2008. Effects of pulling branches on growth and development of apple pear saplings. Inner Mongolia Agric Sci Technol. 57:54–55. https://doi.org/10.3969/j.issn.1007-0907.2008.01.024.

Yang C, Ning D, Shi Z, Ma T, Li Y, Zhang R. 2020. Analysis of fruit growth and development characteristics of olive in Yunnan. Econ For Res. 38:177–183. https://doi.org/10.14067/j.cnki.1003-8981.2020.01.022.

Yin Z. 2002. Logistic curve fitting method. Math Stat Manage 1:41–46. https://doi.org/10.13860/j.cnki.sltj.2002.01.010.

Zhang B, Zheng F, Geng W, Du H, Xiao Y, Peng F. 2023. Effect of branch bending on the canopy characteristics and growth of peach (*Prunus persica* (L.) Batsch). Agronomy. 13(4):1058. https://doi.org/10.3390/agronomy13041058.

Zhen Z, Wang R, Luo S, Xu Y, Hu H. 2024. Effects of different opening angles of apricot and plum on fruit yield and quality. Non-wood For Res. 4:136–144, 154. https://doi.org/10.14067/j.cnki.1003-8981.2024.04.014.